Energetics of Half-Quantum Vortices

K. Roberts[1]
[1]University of Illinois at Urbana-Champaign

Abstract: Magnetic cantilever measurements have detected half-flux states in mesoscopic rings of the layered material Sr_2RuO_4, adding evidence that superconducting Sr_2RuO_4 may be described by a p-wave order parameter. A proposal accounting for this behavior has been presented in which the polarization axis of the condensates lies entirely in the plane. In a half-flux state there is a non-zero polarization, due purely to kinematic effects, which couples to an in-plane magnetic field, lowering the half-flux state's free energy. The viability of such a model and a determination of phenomenological parameters depends heavily on the specific geometry used. A set of Ginzburg-Landau equations has been solved using COMSOL and geometries very similar to the experimental set-up. The results show that the Ginzburg-Landau model can qualitatively reproduce the experimental data within the physically allowable parameter space.

Keywords: superconductivity, multiphysics

1. Introduction

COMSOL has been a useful tool in studying superconductivity[1] due to V.L. Ginzburg and L.D. Landau's phenomenological theory of second order phase transitions[2]. This theory describes superconductivity in terms of an "order parameter" which is the solution of a set of coupled PDEs. Ginzburg-Landau (GL) theory provides a useful explanation to the phenomenon of flux quantization in Type II superconductors in which magnetic flux penetrates the sample in discrete units of ħ/2e.

Experiments performed by Jang et al., at the Univeristy of Illinois at Urbana-Champaign, have explored the existence of half-quantum vortices (HQV) in the layered material Sr_2RuO_4[3] which carry a half unit of magnetic flux. Sr_2RuO_4 is believed to be a spin-triplet p-wave superconductor[4 and references therein] and to exist in the so-called equal spin pairing (ESP) state which can be thought of as consisting of two interacting condensates in the spin configurations $|\uparrow\uparrow>$ and $|\downarrow\downarrow>$.

This suggests that the superconductivity in Sr_2RuO_4 may be modeled using a GL model with two order parameters and appropriate couplings. Solving this model, then, requires the solution of a system of coupled PDEs in a 3-dimensional geometry making COMSOL's advanced FEM solver a natural tool.

In section 2, I will briefly discuss the experimental results which are the motivation for this study. In section 3, I will present an overview of the relevant theory along with the equations used with boundary conditions. In section 4, I will describe the use of COMSOL, detailing specific geometries. Finally, in section 5, I will present results followed by a discussion of their implications.

2. Experimental Results

Originally proposed by Chung, Bluhm, and Kim[6], Jang et al. looked for the existence of half-quantum vortices by manufacturing micron scale rings of Sr_2RuO_4 having the plane of the rings commensurate with the crystal ab-plane (see Figure 1). This geometry serves multiple purposes.

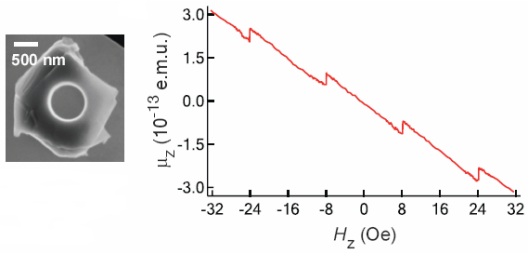

Figure 1. From [3]. A sample of SRO with ring geometry is shown on the left. On the right is the measured magnetic moment along the z-axis versus applied z-axis field at zero in-plane field.

Firstly, spin currents, which do not couple to the magnetic field and are, therefore, not screened in the bulk, are logarithmically divergent in energy with increasing sample size. According to [6], a domain size of order λ, the penetration depth, is necessary for the stabilization of half-quantum vortices. The penetration depth in the ab-plane of Sr_2RuO_4 is 152 nm[4] necessitating mesoscopic domains.

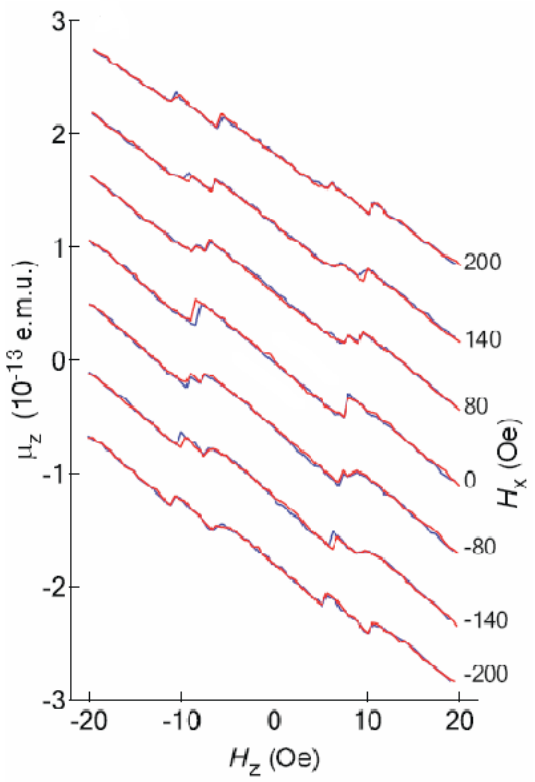

Figure 2. From [3]. The figure shows the magnetic moment versus z-axis field at various in-plane field values. The curves have been offset for easier viewing.

The ring geometry is beneficial as it avoids complications from vortex interactions. When a vortex enters the sample, the flux will simply pass through the center of the ring as opposed to passing through the bulk. This gives a discrete set of vortex states indexed by the quanta of flux passing through the ring.

Using a cantilever magnetometer, Jang et al. were able to measure the magnetic moment of the samples versus applied z-axis field as shown in Figure 1. The negative slope near H_z=0 is indicative of the diamagnetic response of superconductors. The discontinuities in the magnetic moment indicate the entrance of vortices through the sample, the size of the jump proportional to the amount of flux penetrating the sample. The data shown in Figure 1 was taken with zero in-plane field and the discontinuities are believed to be indicative of transitions between integer flux states.

With the application of a non-zero in-plane magnetic field, a separate set of discontinuities appears as shown in Figure 2. It is shown in [3] that these additional transitions are very nearly half as large as the full transitions shown in Figure 1 and are believed to indicate the existence of half-integer flux states. It is of interest to note that the stability region of these half-integer flux states grows linearly with in-plane field and is an important test of our theoretical model.

3. Theoretical Model

3.1 Standard GL theory and flux quantization

The standard GL theory is embodied by the free energy functional

$$F_{GL}[\psi,\mathrm{A}]=\int d^3r\{\frac{1}{2\mathrm{m}}|(-i\hbar\nabla-2e\,\mathrm{A})\psi|^2 +\alpha|\psi|^2+\frac{\beta}{2}|\psi|^4+\frac{1}{2\mu_0}|\mathrm{B}-\mathrm{B}_{app}|^2\}$$

where ψ is the complex scalar order parameter whose squared magnitude represents the density of superconducting charge carriers, **A** is the vector potential with $\mathrm{B}=\nabla\times\mathrm{A}$, e is the fundamental charge, m is a phenomenological mass parameter, and α, β are temperature dependent phenomenological parameters. The GL equations are derived by minimizing the free energy with respect to ψ and **A**. They are:

$$\frac{1}{2\mathrm{m}}(-i\hbar\nabla-2e\,\mathrm{A})^2\psi+\alpha\psi+\beta|\psi|^2\psi=0$$

and

$$\nabla\times\mathrm{B}=\frac{2e}{m}Re\{\psi^*(-i\hbar\nabla-2e\,\mathrm{A})\psi\}$$

The right side of the second equation represents the supercurrent which will vanish within the bulk of the superconductor. In other words:

$$\nabla\psi-\frac{2\mathrm{ie}}{\hbar}\mathrm{A}\psi=0$$

Now consider magnetic flux piercing our superconducting ring and perform a contour integral of the above equation in a closed path, C, around the central hole. Writing $\psi=\rho e^{i\theta}$, choose a path such that ρ is constant. We then arrive at the condition that

$$\int_C \mathrm{A}\bullet dl=n\frac{\hbar}{2e}$$

Thus, the flux passing through our contour is quantized in units of ħ/2e. It was mentioned earlier that the flux states of the ring could be indexed by the number of flux quanta piercing the ring. The number of flux quanta is now seen to be precisely the winding number, n, of the phase of the order parameter around the hole.

For the purposes of numerical calculation, it is customary to use dimensionless units in which the free energy functional takes the form

$$F_{GL}[\psi,\mathbf{A}]=\int d^3r\{|(\frac{\nabla}{\kappa}-i\,\mathbf{A})\psi|^2-|\psi|^2 +|\psi|^4+|\nabla\times\mathbf{A}-\mathbf{B}_{app}|^2\}$$

where $\kappa=(m^2\beta/2\mu_0 e^2\hbar^2)^{1/2}$, the GL parameter, is the ratio of the penetration depth to coherence length in the superconductor. It must be greater than $1/\sqrt{2}$ for Type II behavior. For Sr_2RuO_4 it's value is 2.3[4].

A note should also be made about methods of dealing with the anisotropy of Sr_2RuO_4. In layered materials such as Sr_2RuO_4, gradients of ψ in the z-direction are less energetically expensive than gradients in the ab-plane. This can be taken into account by inserting the tensor diag(1,1,1/γ) into all of the dot products in the free energy with the exception of the last term representing the field energy. For Sr_2RuO_4, the anisotropy parameter γ is 400. For the purposes of this paper I will suppress the appearance of this tensor.

For more information about the de-dimensionalizing procedure or the anisotropic GL theory, see [7].

3.2 GL theory of the ESP state

In the ESP state, there are two order parameters whose squared magnitudes represent the density of the spin-up and spin-down superconducting fluids. Without considering couplings between the two order parameters our model free energy is

$$F_0[\psi_\uparrow,\psi_\downarrow,\mathbf{A}]=F_{GL}[\psi_\uparrow,\mathbf{A}]+F_{GL}[\psi_\downarrow,\mathbf{A}] -|\nabla\times\mathbf{A}-\mathbf{B}_{app}|^2$$

where the subtraction of the last term is to avoid over-counting the field energy.

In our model of the ESP state we consider the addition of a current coupling term

$$F_{CC}[\psi_\uparrow,\psi_\downarrow,\mathbf{A}]=\int d^3r\,\beta\,J_\uparrow\bullet J_\downarrow$$

where β is a material dependent parameter and the **J** are the supercurrents defined by

$$J=Re\{\psi^*(\frac{\nabla}{\kappa}-i\,\mathbf{A})\psi\}\,.$$

In the single condensate model considered in the previous section, the amount of allowed flux quanta was given by the integer winding number, n. In this model, n is replaced by the quantity $(n_\uparrow+n_\downarrow)/2$ involving the winding numbers of the phases of the spin-up and spin-down condensates. The half quantum vortex state is then one where $n_\uparrow+n_\downarrow$ is odd.

The additional current coupling term imposes an energy cost for both superfluids having currents in the same direction. This produces a favoring of the half-flux states over neighboring integer-flux states.

3.3 Kinematic Spin Polarization

Making a connection with fluid mechanics, the GL equation for ψ can be viewed as a Bernoulli equation for the superfluid. There is a reduction of superfluid density $|\psi|^2$ with increasing superfluid velocity, **grad**(θ)/κ-**A**. A mismatch in superfluid velocities between the spin-up and spin-down condensates would then lead to a difference in their densities and, thus, a spin polarization. The magnetic moment resulting from this spin polarization would couple to an in-plane field and reduce the state's energy.

This is precisely what happens in the the half-flux state. Since, in the half-flux state, the winding numbers of the spin-up and spin-down condensates are necessarily not equal, their velocities will be different, as well (Figure 3). This additional magnetic moment only exists, then, in the half-integer state and, thus, provides the half-integer state a reduction in free energy that grows with in-plane fields.

To embody this behavior we add the additional term

$$F_{HI}[\psi_\uparrow,\psi_\downarrow,\mathbf{A}]=\int d^3r\,\mu_{HI}(|\psi_\uparrow|^2-|\psi_\downarrow|^2)\,B_{ab}$$

to our free energy with the difference in the densities of the spin-up and spin-down condensates coupled to the in-plane component of the magnetic field. The strength of this term will be determined by the size of the parameter μ_{HI}.

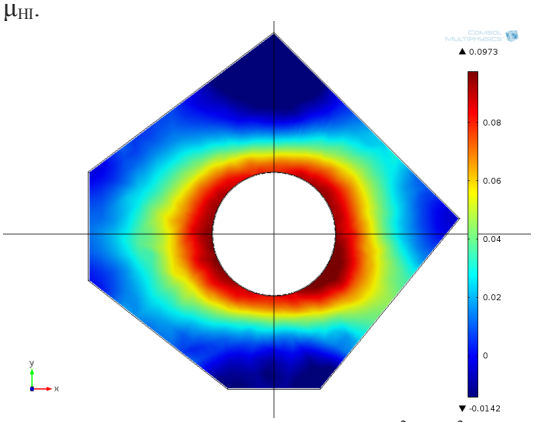

Figure 3. A COMSOL solution of $|\psi_\uparrow|^2$- $|\psi_\downarrow|^2$ in the $(n_\uparrow,n_\downarrow)=(0,1)$ state for a sample ring geometry.

4. Use of COMSOL Multiphysics

The simulation geometry is shown in Figure 4. In dimensionless units, distances are measured in terms of the ab-plane penetration depth λ. The superconducting ring's inner radius is 2λ while the outer radius averages 4.25λ. The height of the sample is 3λ. This roughly matches the experimental sample shown in Figure 1.

The superconducting ring was placed in a surrounding spherical volume with a radius of 15λ. This radius was chosen to balance competing effects of increased computation time for larger radii and spuriously high free energies in higher flux states for smaller radii.

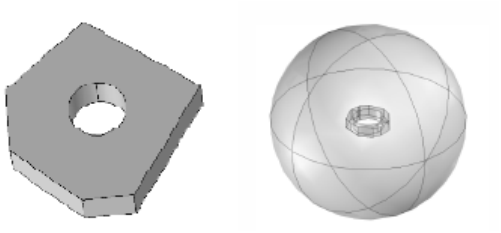

Figure 4. On the left is shown the simulated geometry for the superconducting ring (compare to sample in Figure 1). On the right is shown a ring embedded in the total spherical volume.

Using notation from section 3, the total model free energy is given by

$$F_{tot}[\psi_\uparrow, \psi_\downarrow, \mathrm{A}] = F_0 + F_{cc} + F_{HI} \quad .$$

Our method for exploring the energetics of the half- and integer-flux states was to use a relaxation technique where we set the initial conditions such that the system was in the desired flux state. For instance, if it was desired to solve for the fields in a $(n_\uparrow, n_\downarrow)=(1,0)$ state one would set the initial conditions of the order parameters to be

$$\psi_\uparrow(t=0) = \exp\{i\theta\}, \psi_\downarrow(t=0) = 1 \quad .$$

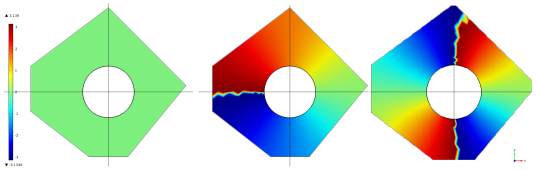

Figure 5. Plots of the phase of the order parameter for winding numbers of zero, one, and two.

The initial conditions for the vector potential were chosen so as to produce the desired applied magnetic field.

The boundary conditions for the spin-up and spin-down order parameters are derived, in the usual way, by forcing the surface terms that arise in varying the free energy to vanish. Physically, they ensure that the currents are not normal to the surface so the condensate does not leave the superconducting ring.

The integral of the vector potential is over the entire volume so it's boundary condition is applied on the edge of the total volume. There was applied a Dirichlet boundary condition, setting the vector potential equal to the same function as was used for the initial conditions, ensuring a fixed flux through the volume.

We then solved the equations

$$\frac{\partial \psi_\uparrow^*}{\partial t} = \frac{-\delta F}{\delta \psi_\uparrow^*}, \frac{\partial \psi_\downarrow^*}{\partial t} = \frac{-\delta F}{\delta \psi_\downarrow^*}, \frac{\partial \mathrm{A}}{\partial t} = \frac{-\delta F}{\delta \mathrm{A}}$$

using a time-dependent study for 20 time units to allow the system to relax into it's equilibrium state.

Once an equilibrium solution was reached, the free energy was calculated by performing the appropriate volume integral. By doing this for desired values of the magnetic field, one could construct the functional form of free energy versus applied z-axis field for various values of in-plane field.

5. Results

Figure 6 shows some results of the free energy of the system versus applied z-axis field (from 0 to 40 Gauss) for a few values of applied in-plane magnetic field. The blue line depicts the (0,0) and (1,1) integer-flux states while the red line depicts the (1,0) half-flux state. The data for each value of in-plane field has been shifted by a constant so that the integer-flux state's data overlap one another. The dimensionless parameter values used here are β=0.7 and μ=0.75.

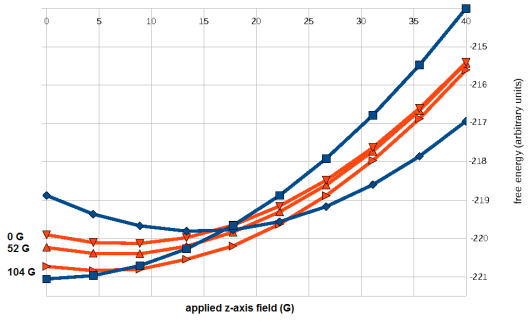

Figure 6. Free energy diagram showing the growing stability of the half-flux state with increasing magnetic field.

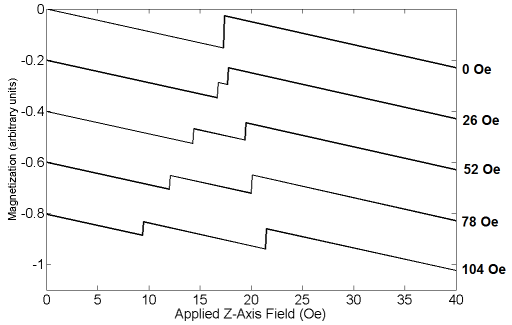

Figure 7. Magnetization curves for the geometry of Figure 4 with β=0.69 and μ=0.7.

One can see from the diagram that the half-flux state has a reduced free energy versus the integer-flux states for higher values of in-plane field.

Applying a parabolic fit to the free energy curves, one can take the the derivative with respect to the applied magnetic field to obtain the magnetization curves. Figure 7 displays magnetization curves versus z-axis field for various values of in-plane field as in Figure 2. The magnetization curves are seen to be qualitatively similar. By adjusting β and μ_{HI} one may obtain the desired minimum in-plane stabilization field and stability region growth rate. The data in Figure 7 was produced with the geometry shown in Figure 4 with β=0.69 and μ=0.7.

The size of the stability region versus applied in-plane magnetic field of the magnetization curves in Figure 7 is plotted in Figure 8. The growth rate has a very good linear fit. With this choice of parameters and geometry, the minimum in-plane field necessary to stabilize the HQV is approximately 17.4 Oe while the growth rate is 0.14.

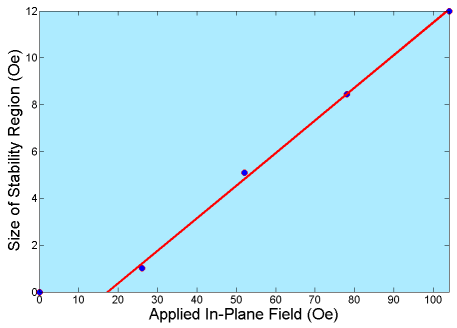

Figure 8. Plot of the linear growth of the stability region.

6. Discussion

In the results section, it was seen that the theoretical model proposed can reproduce the data and obtain order of magnitude estimates for the phenomenological model parameters. Accurate determination of β and μ and a construction of an accurate phase diagram are problematic due to different growth rates and minimum stabilizing in-plane fields across experimental samples. This is most likely due to inaccuracies in modeling the superconducting volume. Due to being damaged during construction, the entire ring is not superconducting and determining the superconducting portion is not technically possible, at this time. This is made abundantly clear by the difference between the periodicity of the experimental and simulated sample discussed in this paper. From Figure 1, the transition from the zero to first integer flux state occurs at approximately 8 Gauss. From Figure 6, the simulated geometry's transition occurs at approximately 17 Gauss. This is indicative of the simulated ring having a smaller internal radius which could be explained by the experimental sample's inner edge being damaged and unable to enter the superconducting state.

Work is currently being done to increase the available data in order to determine, more accurately, the phenomenological parameter values and the sensitivity of the system's behavior to changes in those values as well as the system's geometry.

7. References

1. T.S. Larson., M.P. Sorensen, N.F. Pedersen, S. Madsen, The Ginzburg-Landau Equation Solved by the Finite Element Method. In: *Proc. 2006 Nordic COMSOL Conference.* (2006)

2. V.L. Ginzburg and L.D. Landau, On the Theory of Superconductivity, *Zh. Eksp. Teo. Fiz.,* **20**, 1064 (1950)

3. J.Jang, et al, Observation of half-height magnetization steps in Sr_2RuO_4, *Science*, **331**, 6014 (2011)

4. A.P. Mackenzie, Y. Meano, The superconductivity of Sr_2RuO_4 and the physics of

spin-triplet pairing, *Rev. Mod. Phys.*, **75**, 657 (2003)

5. V. Vakaryuk, A.J. Legget, Spin polarization of half-quantum vortex in systems with equal spin pairing, *Phys. Rev. Lett.*, **103**, 057003 (2009)

6. S.B. Chung, H. Bluhm, E.-A. Kim, Stability of half-quantum vortices in p_x+ip_y superconductors. *Phys. Rev. Lett.* **99**, 197002 (2007)

7. S. Jonathan Chapman, Qiang Du, Max D. Gunzburger, On the Lawrence-Doniach and Anisotropic Ginzburg-Landau Models for Layered Superconductors. *SIAM J. Appl. Math*, **55**, 1 (1995)

8. Acknowledgements

I would like to thank Anthony Leggett, Michael Stone, Raffi Budakian, David Ferguson, and Victor Vakaryuk for their valuable insights and suggestions.